

# 一种改进的微组装焊点三维重建算法

赵辉煌<sup>1,2</sup>, 王耀南<sup>1</sup>, 孙雅琪<sup>2</sup>, 魏书堤<sup>2</sup>

(1. 湖南大学 电气与信息工程学院, 长沙 410082; 2. 衡阳师范学院 计算机科学系, 衡阳 421008)

**摘 要:** 焊点表面三维重建是微组装质量三维检测与控制技术的重点研究内容之一。焊点图像中存在的高亮区, 使得微电子组装焊点表面三维重建成为难点问题。为解决此问题, 通过分析焊点表面光照反射项, 结合焊点图像的特点, 依据光照反射原理, 推导焊点表面反射光照反射模型; 通过分析图像中高亮区的形成原理, 提出一种改进的微组装焊点表面三维重建算法。结果表明, 与基于其它传统光照反射模型的三维重建方法相比, 采用提出的三维重建算法可解决微组装焊点三维重建失真问题, 重建出的焊点三维形状更加理想。

**关键词:** 焊点; 微电子组装; 三维重建; 阴影恢复形状算法

**中图分类号:** TG 409 **文献标识码:** A **文章编号:** 0253-360X(2014)08-0030-05

## 0 序 言

微电子组装(以下简称微组装)是采用微电子技术或混合微电子技术在电路板上将芯片、微小型元器件等用微细焊接技术形成微电子组装模块的工艺技术。微组装技术在航空、航天和船舶等平台的电子装备上得到了广泛的应用<sup>[1-2]</sup>。由微组装技术形成的电路模块的焊点, 一般是指元器件焊脚与印制电路板(printed circuit board, PCB)焊盘焊接结合处熔融钎料。焊点具有保障电气性能畅通和机械连接可靠的特征。统计分析表明, 微电子组装电路模块产品质量缺陷的80%都是由焊点质量缺陷所引起的。在电子产品组装过程中及时检测、发现焊点组装不良现象, 对提高微电子组装电子产品组装质量和保障产品可靠性最为重要。研究微组装焊点三维重建技术, 有利于指导改善微组装焊点质量及其焊接工艺, 提高焊点质量自动检测能力, 同时推动焊点质量三维智能鉴别技术的发展<sup>[3-4]</sup>。

采用阴影恢复(SFS)方法对微组装焊点进行表面三维重建, 此方法具有重建速度快、成本低和实时性高等特点。但在采用SFS方法进行微组装焊点重建过程中, 由于物体表面可能存在镜面反射的原因, 图像中存在高亮区, 这些高亮区严重影响了三维重建的结果。而对于图像中的高亮区, 产生原因有多

种。例如焊点表面镜面反射产生的高亮区, 或是焊盘表面反射产生高亮区等, 可能会带来重建结果失真的问题<sup>[5-6]</sup>。采用传统的基于SFS原理的方法不能很好地解决由此带来的三维重建问题。为解决此问题, 提出一种改进的微组装焊点表面三维重建算法。

## 1 微组装焊点表面三维重建基本原理

微组装焊点表面三维重建具体方法是利用专业的焊点图像采集系统, 视频捕捉元器件焊点2D图像。只需获取单幅焊点图像, 采用相应的图像处理技术对微组装焊点图像进行处理。由于传统的光照反射模型未考虑焊点自身特点, 精度不高, 使得微组装焊点三维重建精度很受影响。依据光照原理, 从分析焊点表面光照反射项入手, 研究焊点表面及焊点图像的特点, 针对由焊点表面镜反射引起的高亮区而产生的重建精度不高问题, 提出一种新的焊点表面光照反射模型, 并通过设定相关约束条件, 采用SFS线性化方法对光照模型进行求解。针对其它原因引起的高亮区而产生的重建失真问题, 提出一种基于剖面检测的重建结果修正算法。最后重建出微组装焊点表面三维形状。基本原理如图1所示。

## 2 微组装焊点表面光照反射模型

### 2.1 微组装焊点表面光照反射模型推导

光照反射模型是根据光学物理有关定律, 用来计算物体表面上任意一点投向观察者眼中的光亮度大小和色彩组成的数学公式, 它用来描述光照射到

收稿日期: 2013-02-19

基金项目: 国家高技术研究发展计划资助项目(863计划, 2007-AA04Z244); 湖南省自然科学基金资助项目(12JJ4058); 湖南省“十二五”重点建设学科资助项目; 湖南省科技厅资助项目(2010FJ4077, 2013GK3064, 2013GK3082)

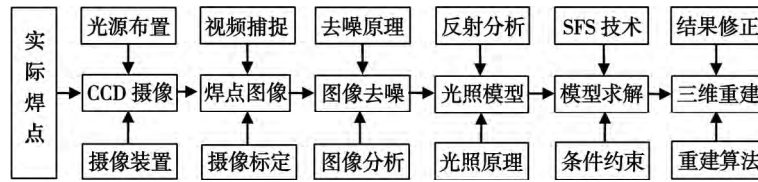


图 1 微电子组装焊点表面三维重建基本原理

Fig. 1 Process of 3D reconstruction algorithm for microelectronics assembly Solder Joint

物体表面发生的反射、折射和吸收等物理现象<sup>[7,8]</sup>。对于微组装焊点,其具有两个显著特点:(1)焊点由同一种成分的焊膏焊接而成,多数是合金材料;(2)焊点表面会引起镜面反射。这些特点使得基于光照反射模型的传统重建算法较难直接应用于焊点的三维重建。针对这两个特点,研究一种适合于微组装焊点表面三维重建的光照反射模型。在现有的光照反射模型中,典型的漫反射光照反射模型有 Oren - Nayar 模型<sup>[9,10]</sup>,其模型公式为

$$L_d(\theta_r, \theta_i, \psi_r, \psi_i, \sigma) = \rho L_i \cos \theta_i \{ A + B [0.4 \cos(\psi_r - \psi_i)] \sin \alpha \tan \beta \} / \pi \quad (1)$$

式中:  $A = 1 - 0.5\sigma^2 / (\sigma^2 + 0.33)$ ;  $B = 1 - 0.45\sigma^2 / (\sigma^2 + 0.99)$ ;  $\sigma$  是高斯分布的标准方差,由物体表面粗糙度确定;  $\rho$  是表面反射率;  $L_i$  是入射光强度;  $\alpha = \max[\theta_r, \theta_i]$ ;  $\beta = \min[\theta_r, \theta_i]$ ;  $\theta_i$  是法线与入射光线的夹角;  $\theta_r$  是法线与视觉方向的夹角;  $\psi_r$  是入射光线在平面上的投影与法平面的夹角;  $\psi_i$  是视觉方向在平面上的投影与法平面的夹角。Oren - Nayar 模型在重构粗糙表面的物体时,具有较高的重构精度。

Torrance - Sparrow 假设物体表面平面斜率的分布函数满足高斯分布,从而推导出一个简化的镜面反射光照模型<sup>[11]</sup>,其模型公式为

$$L_s = G_s L_i \rho e^{-(\varphi/\sigma)^2} / \pi \quad (2)$$

式中:  $G_s$  是几何衰减因子,取值范围是  $[0.8, 1]$ ;  $\varphi$  是表面微平面的法线  $N$  方向与表面平均法向量的夹角,即  $\varphi = \arccos(NH)$ ; 单位向量  $H$  可近似表达为  $H = 0.5 \times (V + L)$ ,其中  $V$  是视觉方向单位向量;  $L$  是光源方向单位向量。

由于焊点由合成金属材料融化而成,焊点表面除了漫反射,还存在镜面反射。因此分别对式(1)镜面反射分量和式(2)漫反射分量进行线性叠加,得到微组装焊点表面光照强度( $I$ )模型,即

$$I = K_s L_s + K_d L_d = L_i K_s \rho G_s e^{-(\varphi/\sigma)^2} / \pi + L_i K_d \rho \cos \theta_i \{ A + B [0.4 \cos(\psi_r - \psi_i)] \sin \alpha \tan \beta \} / \pi \quad (3)$$

式中:  $L_d$  和  $L_s$  分别表示漫反射光强度和镜面反射光

强度;  $K_d$  和  $K_s$  是反射分量系数。对于式(3),求解比较复杂,需要做必要的简化。在一般情况下,由于在微组装焊点图像拍摄过程中,拍摄方向和光源方向是同一个方向,则  $\alpha = \beta = \theta_i = \theta$ ,对式(1)进行改进,化简为

$$L_d(\theta, \sigma) = \rho L_i (A \cos \theta + B \sin^2 \theta) / \pi \quad (4)$$

则式(3)可以简化

$$I = K_s L_s + K_d L_d = L_i K_s \rho G_s e^{-(\varphi/\sigma)^2} / \pi + L_i K_d \rho (A \cos \theta + B \sin^2 \theta) / \pi \quad (5)$$

式(5)可以根据不同类型焊点表面的粗糙度和表面反射率确定,但需要满足条件  $K_d + K_s = 1$ 。

## 2.2 微组装焊点表面光照反射模型求解

光照反射模型 SFS 求解算法有最小化方法、局部分析法和线性化法等。其中线性化方法具有求解简单和求解速度快的特点。文中采用线性化方法对改进光照反射模型求解,以表面点坐标梯度为变量,设  $(-p, -q, 1)$  是物体表面点的方向向量,  $p = \frac{\partial z}{\partial x}$ ,  $q = \frac{\partial z}{\partial y}$ ,  $(-p_0, -q_0, 1)$  是光源方向向量。为了提高线性化函数中高度值的精度,采用迭代法求解,得到焊点表面任意点  $(x, y)$  的高度迭代公式,即

$$Z^n(x, y) = Z^{n-1}(x, y) + \frac{-f(Z^{n-1}(x, y))}{\frac{d}{dZ}(x, y) f[Z^{n-1}(x, y)]} \quad (6)$$

式中:  $f$  是式(5)所对应的函数表达式;  $Z$  为重建高度;  $Z^{n-1}(x, y)$ ,  $Z^n(x, y)$  分别代表第  $n-1$  次和第  $n$  次迭代法结果,且

$$\frac{d}{dZ}(x, y) f[Z^{n-1}(x, y)] = - \left( (A - 2B \cos(\theta)) L_i K_d D_d + L_i K_s \frac{\rho}{\pi} G_s \frac{2\varphi}{\sigma^2} e^{-(\varphi/\sigma)^2} D_s \right) \quad (7)$$

$$D_d = \frac{p_0 + q_0}{\sqrt{p_0^2 + q_0^2 + 1} \sqrt{p^2 + q^2 + 1}} - \frac{(p + q)(pp_0 + qq_0 + 1)}{\sqrt{p_0^2 + q_0^2 + 1} \sqrt{(p^2 + q^2 + 1)^3}} \quad (8)$$

$$D_s = \frac{1}{\sqrt{1 - (NH)^2}} \left( \frac{(p_0 + q_0)(1 + p^2 + q^2) - (p + q)(1 + p_0p + q_0q)}{\sqrt{1 + p_0^2 + q_0^2} \sqrt{(p^2 + q^2 + 1)^3}} \right) \quad (9)$$

式中:  $NH$  分别为  $N(-p, -q, 1)$ ,  $H(-p_0, -q_0, 1)$  且

$$NH = \frac{1 + p_h p + q_h q}{\sqrt{1 + p^2 + q^2} \sqrt{p_h^2 + q_h^2 + 1}} \quad (10)$$

### 3 微组装焊点三维重建算法改进

#### 3.1 焊点表面三维重建改进算法原理

通过以上改进光照反射模型的推导可知,当图像中存在由焊点表面镜面反射造成的高亮区时,采用改进光照反射模型提高焊点表面三维重建的精度.但对于图像中存在的非焊点表面镜面反射产生

的高亮区(如焊盘表面反射引起),由于产生原理完全不一样,无法采用提高光照反向模型的精确来解决.结果表明,得到的三维重建结果会发生失真现象,很不理想.针对这一问题,研究一种改进算法,通过对生成高亮区的原因分析,提出一种基于剖面检测的焊点表面三维形状重建修正算法.

三维重建结果修正算法主要由三部分组成,(1)对三维重建后的结果进行切分,判断高亮区的位置;(2)通过判断点的高度值,判断这些点是否为焊点表面上的点,进而判断高亮区是否是由焊点表面的镜面反射产生的;(3)焊点高度修正.对于焊点表面上的点,在焊点表面光照反射模型中已加以考虑,不必修改;但对于非焊点表面上点,高度值越大,代表对应的焊点图像上焊料越少或没有焊料,则重建高度越小.基本原理如图2所示.图2中修正参数的设置应考虑焊点类型,并且参数的大小通过经验来调整.

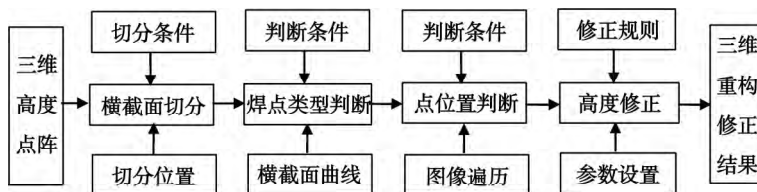


图2 焊点表面三维重构修正算法基本原理

Fig. 2 Process of 3D reconstruction amending for microelectronics assembly solder joint

#### 3.2 焊点表面三维重建改进算法流程

根据焊点表面三维重建结果修正基本原理,设计相应的焊点表面三维重建结果修正算法,算法流程如图3所示.

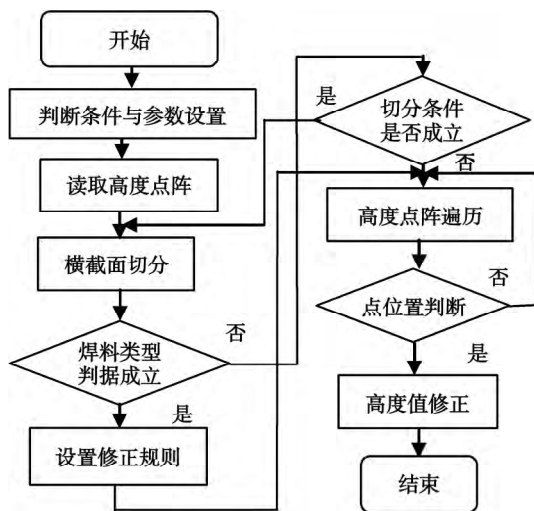


图3 微电子组装焊点三维重建修正算法

Fig. 3 Amending algorithm for microelectronics assembly Solder Joint 3D

### 4 微组装焊点三维重建试验结果比较

为比较提出的方法与传统方法三维重建的效果,通过焊点图像采集系统分别采集两类存在高亮区的焊点图像,分别是(1)焊点表面高亮区是由焊点表面镜面反射形成的;(2)焊点表面高亮区是由其它原因反射形成的.如图4中的右焊点,图像的高亮区由焊点表面镜面反射形成的.分割出右焊点,如图5所示.针对表面高亮区是由焊点镜面反射而产生的,文中已通过设置镜面反射系统来提高重构的效果.

采用文献[12]提出的去噪算法去除图5中的噪声,再依据得到的去噪结果,分别采用 Lambert 光照反射模型和 Oren - Nayar 光照反射模型进行三维

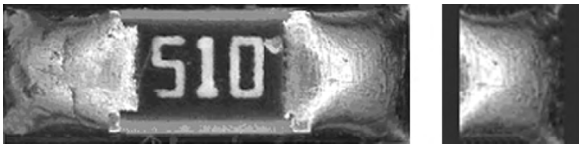


图 4 元件及焊点图像

Fig. 4 Solder joint and components

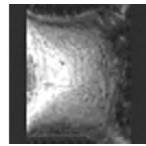


图 5 焊点图像

Fig. 5 Solder joint

重建试验, 得到重建结果分别如图 6a 和图 6b 所示, 采用改进的算法重建结果如图 6c 所示.

为比较重建结果, 获取三个不同重建结果的中间剖面, 如图 7 所示. 图 7a, b 分别为采用 Lambert 光照模型和 Oren - Nayar 光照反射模型重建结果中间剖面, 图 7c 为采用改进算法重建结果中间剖面.

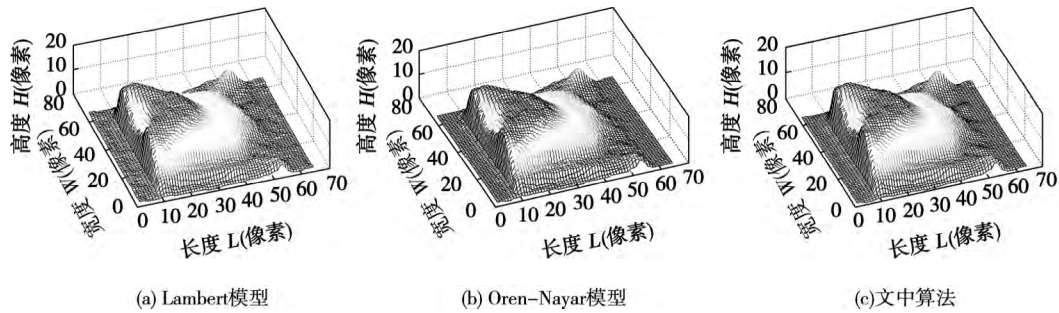


图 6 微组装焊点三维重建试验结果图像比较

Fig. 6 Solder joint 3D reconstruction results comparison based on different method

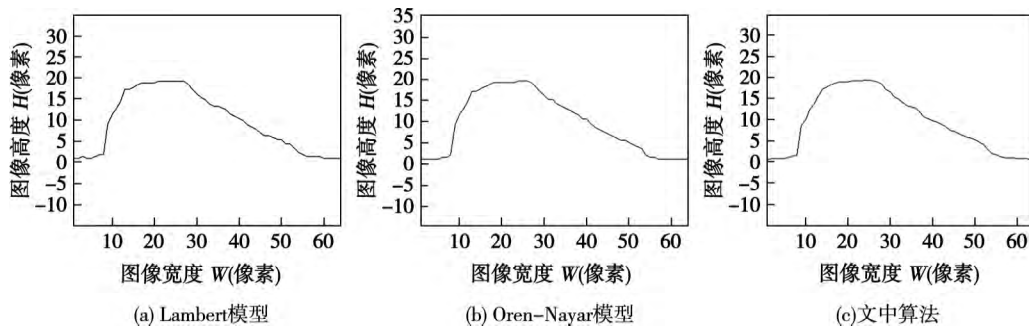


图 7 微组装焊点三维重建结果中间剖面比较

Fig. 7 Middle section results comparison in of 3D reconstruction

通过图 7 结果比较可发现, 基于改进算法得到的中间剖面的曲线更加连续, 表面高度变化更加平缓, 效果最好.

获取到焊料不足焊点和元件图像如图 8 所示, 对于图 8 中的左焊点中的高亮区, 由于焊盘的镜面反射产生的分割出左焊点, 如图 9 所示.



图 8 焊料不足元件及焊点图像

Fig. 8 Insufficient solder joint and components

图 9 焊料不足焊点图像

Fig. 9 Insufficient solder joint

照反射模型得到三维重建结果如图 10a 所示, 采用 Oren - Nayar 光照反射模型得到三维重建的结果如图 10b 所示, 两个重建结果产生了失真现象. 采用改进的算法重建焊点表面三维形状, 结果如图 10c 所示.

三维重建结果对应的中间剖面如图 11 所示. 图 11a, b 分别为采用 Lambert 光照反射模型和 Oren - Nayar 光照模型重建结果中间剖面, 图 11c 为采用改进算法重建结果中间剖面.

通过图 10 和图 11, 可得出 (1) 对于图像的高亮区, 不是由于焊点表面的镜面反射产生, 采用 Lambert 光照反射模型和 Oren - Nayar 光照反射模型, 重建结果发生了失真; (2) 采用改进算法得到的重建结果比较合理, 三维形状中间剖面曲线连续, 解决了由于焊点图像中存在非焊点表面镜面反射产生的高亮区所带来的失真问题.

对焊点图像进行去噪处理后, 采用 Lambert 光

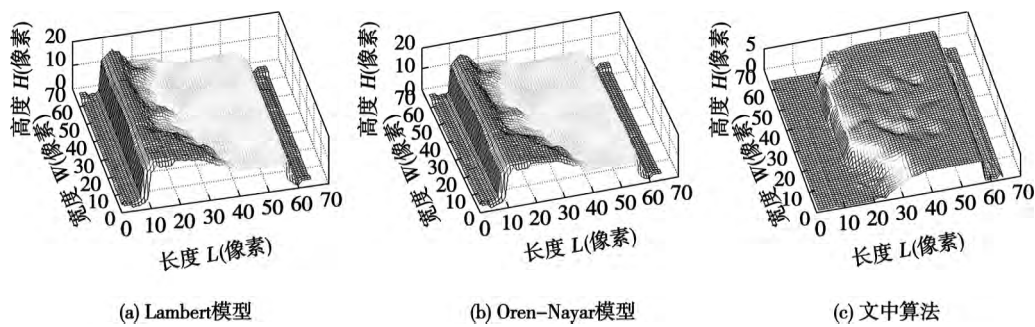


图10 去噪处理后微组装焊点三维重建试验结果比较

Fig. 10 Solder joint 3D reconstruction results comparison based on different method after de-noising processing

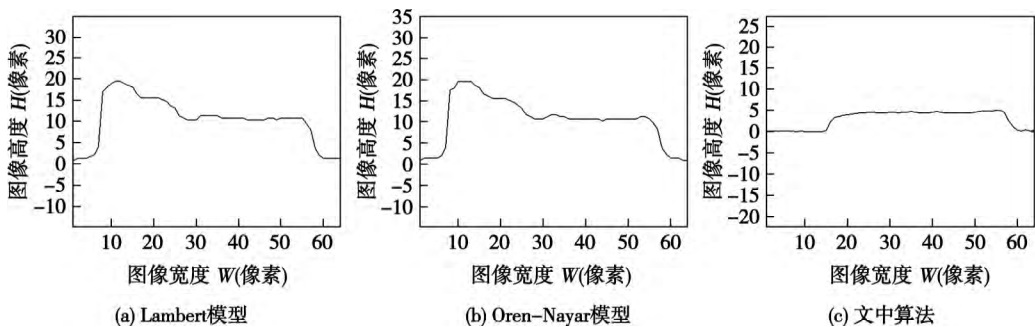


图11 去噪处理后微组装焊点三维重建结果中间剖面比较

Fig. 11 Middle section results comparison of 3D reconstruction after de-noising processing

## 5 结 论

(1) 当焊点表面的高亮区由焊点表面镜面反射产生时,提出微组装焊点表面光照反射模型,增加镜面反射分量,提高重构的精度。

(2) 当焊点表面的高亮区不是由表面镜面反射产生时,提出一种基于剖面检测的重建结果修正算法,解决采用SFS方法重构结果失真的问题,提高三维重建的效果。

### 参考文献:

- [1] 张为民,郑红宇,严伟. 电子封装与微组装密封的特点及发展趋势[J]. 国防制造技术, 2010, 2(1): 60-62.  
Zhang Weimin, Zheng Hongyu, Yan Wei. Characteristics and development trend of the electronic packaging and micro-assembly sealed [J]. Defense Manufacturing Technology, 2010, 2(1): 60-62.
- [2] 周德俭,黄春跃,吴兆华,等. SMT焊点虚拟成形和SMT产品虚拟组装技术研究[J]. 计算机集成制造系统, 2006, 12(8): 1267-1272.  
Zhou Dejian, Huang Chunyue, Wu Zhaohua, et al. SMT solder joints quality assurance based on solder joints virtual evolving technology [J]. Computer Integrated Manufacturing Systems, 2006, 12(8): 1267-1272.
- [3] 张瑞秋,张宪民,陈忠. 基于三维X射线和Fisher准则的BGA焊点检测算法[J]. 焊接学报, 2011, 32(11): 59-63.  
Zhang Ruiqiu, Zhang Xianmin, Chen Zhong. BGA solder joint inspection algorithm based on 3D X-ray and Fisher criterion [J]. Transactions of the China Welding Institution, 2011, 32(11): 59-63.
- [4] 尹立孟, Michael Pecht, 位松, 等. 焊点高度对微尺度焊点力学行为的影响[J]. 焊接学报, 2013, 34(8): 27-32.  
Yin Limeng, Michael Pecht, Wei Song, et al. Effect of joint height on the mechanical behaviors of micro scale solder joints [J]. Transactions of the China Welding Institution, 2013, 34(8): 27-32.
- [5] Li Junhui, Liu Linggang, Deng Luhua, et al. Interfacial microstructures and thermodynamics of thermosonic Cu-wire bonding [J]. IEEE Electron Device Letters, 2011, 32(10): 1433-1435.
- [6] Said A F, Bennett B L, Karam L J, et al. Automated detection and classification of non-wet solder joints [J], IEEE Transactions on Automation Science and Engineering, 2011, 8(1): 67-80.
- [7] 何炳蔚, 陈志鹏, 林东艺, 等. 融合SFS和主动视觉技术的未知物体重建方法[J]. 仪器仪表学报, 2012, 33(4): 727-736.  
He Bingwei, Chen Zhipeng, Lin Dongyi, et al. Research on reconstruction method for unknown objects through incorporating SFS algorithm and active vision technology [J]. Chinese Journal of Scientific Instrument, 2012, 33(4): 727-736.

(3) 通过与试验数据比较,经修正后的振动疲劳 S-N 曲线具有较高的准确性。

#### 参考文献:

- [1] 吴良晨,王东坡,邓彩艳,等. 超长寿命区间 16Mn 钢焊接接头疲劳性能[J]. 焊接学报,2008,29(3): 117-120.  
Wu Liangchen, Wang Dongpo, Deng Caiyan, *et al.* Fatigue properties of welded joints of 16Mn steel in super long life region [J]. Transactions of the China Welding Institution, 2008, 29(3): 117-120.
- [2] 方冬慧,刘永杰,陈直言,等. Q345 桥梁钢焊接接头超高周疲劳性能[J]. 焊接学报,2011,32(8): 77-80.  
Fang Donghui, Liu Yongjie, Chen Yizhan, *et al.* Ultra-high cycle fatigue behavior of Q345 bridge steel welded joint [J]. Transactions of the China Welding Institution, 2011, 32(8): 77-80.
- [3] 王 弘,高 庆. 超声疲劳试验中载荷频率对材料疲劳性能的影响[J]. 理化检验-物理分册,2005,41(9): 433-435.  
Wang Hong, Gao Qing. Effect of load frequency on fatigue behavior of material in ultrasonic fatigue testing [J]. PYCA (Part: a physicstest test), 2005, 41(9): 433-435.
- [4] 闫桂玲,王 弘,高 庆. 超声频率加载下 50 车轴钢超长寿命疲劳性能研究[J]. 中国铁道科学,2004,25(2): 78-81.  
Yan Guilin, Wang Hong, Gao Qing. On ultra-long life fatigue behavior of 50 axle steel under ultrasonic frequency [J]. China Railway Science, 2004, 25(2): 78-81.
- [5] 薛红前,陶 华. 20 kHz 频率下高强度钢超高周疲劳研究[J]. 机械工程材料,2005,29(5): 12-15.  
Xue Hongqian, Tao Hua. Super high cycle fatigue of high strength steels at a frequency of 20 kHz [J]. Materials for Mechanical Engineering, 2005, 29(5): 12-15.
- [6] 尹丹青,王东坡,刘 哲. Q235 钢和 16Mn 钢接头超长寿命疲劳行为及疲劳寿命设计[J]. 天津大学学报,2009,42(6): 513-517.  
Yin Danqing, Wang Dongpo, Liu Zhe. Ultra-long life fatigue behavior and fatigue life design of joint between steel Q235 and steel 16Mn [J]. Journal of Tianjin University, 2009, 42(6): 513-517.
- [7] 彭修宁,韦斌凝,薛建阳. 产生坑蚀后建筑用钢筋 S-N 曲线中 C 参数劣化规律的研究[J]. 西安建筑科技大学学报,2009,41(5): 627-630.  
Peng Xiuning, Wei Binning, Xue Jianyang. Study on the deterioration of parameter C in S-N curve of steel bars with corrosion-pits used in construction [J]. Journal of Xi'an University of Architecture & Technology, 2009, 41(5): 627-630.
- [8] Suresh S. 材料的疲劳[M]. 王中光,译. 北京: 国防工业出版社,1993.
- [9] Hobbacher A. Recommendations for fatigue design of welded joints and components [M]. German: International Institute of Welding, 2002.
- [10] 吴良晨. 超声频分量双周疲劳载荷作用下焊接接头的疲劳性能[D]. 天津: 天津大学,2008.

**作者简介:** 范文学,男,1981 年出生,博士研究生,讲师. 主要从事焊接疲劳和数控加工方面的科研和教学工作. 发表论文 5 篇.  
Email: fw201878@163.com

**通讯作者:** 陈芙蓉,女,教授. Email: cfr7075@163.com

#### [上接第 34 页]

- [8] Ruo Zhang, Ping Sing Tsai, James Edwin Cryer, *et al.* Shape from shading: a survey [J]. IEEE Transactions on Pattern Analysis and Machine Intelligence, 1999, 21(8): 119-131.
- [9] Habert S. A novel method for an automatic 3D reconstruction of coronary arteries from angiographic images [C] // 2012 11th International Conference on Information Science, Signal Processing and their Applications (ISSPA), Montréal, QC, Canada, 2012: 484-489.
- [10] Oren M, Nayar S K. Generalization of Lambert's reflectance model [C] // Proceedings of the 21st Annual Conference on Computer Graphics and Interactive Techniques, New York, 1994: 239-246.
- [11] Cook R L, Torrance K E. A reflectance model for computer graphics [J]. Computer Graphics, 1981, 15(3): 307-316.
- [12] 赵辉煌,周德俭,吴兆华,等. 基于小波包变换与自适应阈值的 SMT 焊点图像[J]. 焊接学报,2011,32(11): 73-76.  
Zhao Huihuang, Zhou Dejian, Wu Zhaohua, *et al.* SMT solder joint image denoising based on wavelet packet transform and adaptive threshold [J]. Transactions of the China Welding Institution, 2011, 32(11): 73-76.

**作者简介:** 赵辉煌,男,1982 年出生,博士,副教授. 主要从事计算机视觉、三维重建、图像处理、微电子组装检测等方面研究. 发表论文 30 余篇. Email: betterlife008@163.com

### Hot corrosion resistance of plasma-sprayed MCrAlY coatings by laser remelting on TiAl alloy surface

WANG Dongsheng<sup>1,2</sup>, TIAN Zongjun<sup>1</sup>, SHEN Lida<sup>1</sup>, HUANG Yinhui<sup>1</sup> (1. College of Mechanical and Electrical Engineering, Nanjing University of Aeronautics and Astronautics, Nanjing 210016, China; 2. College of Mechanical Engineering, Tongling University, Tongling 244000, China). pp 17 – 20

**Abstract:** The MCrAlY coatings were prepared by plasma spraying on TiAl alloy surface, laser remelting experiment had been carried out and the hot corrosion resistance of TiAl alloy, plasma-sprayed and laser-remelted MCrAlY coatings in 5% Na<sub>2</sub>SO<sub>4</sub> + 25% NaCl (mass fraction) molten salt at 850 °C were researched. The hot corrosion failure mechanisms of three kinds of materials were analyzed and the influence of laser remelting on hot corrosion behavior of plasma-sprayed MCrAlY coating were discussed. The results show that the plasma-sprayed MCrAlY coating has better oxidation resistance than the original TiAl alloy, and the laser-remelted coating has the best oxidation resistance. The hot corrosion of MCrAlY coating included surface oxidation and internal sulfide, and produced Al<sub>2</sub>O<sub>3</sub>, Cr<sub>2</sub>O<sub>3</sub>, NiO, NiCr<sub>2</sub>O<sub>4</sub>, Ni<sub>3</sub>S<sub>2</sub> and CrS et al.

**Key words:** laser remelting; plasma spraying; MCrAlY coating; TiAl alloy; hot corrosion resistance

### Experiment on metal transfer control of laser enhanced GMAW welding

ZHU Jialei, JIAO Xiangdong, QIAO Xi, JIA Cunfeng (Mechanical Engineering College, Beijing Institute of Petrochemical Technology, Beijing 102600, China). pp 21 – 24, 29

**Abstract:** Underwater ambient pressure has negative effect on metal transfer and welding processing stability, so extra force is needed to help to stabilize welding arc and improve metal transfer state during underwater welding. To verify the feasibility of laser which enhanced metal transfer control, the related experiment system was built at atmospheric pressure, and contrastive study on metal transfer state with and without laser enhanced was conducted. Results showed that the application of a certain power density of laser could improve metal transfer behavior obviously and the size of droplet could be controlled by laser, the welding stability also could be improved. The result laid a foundation for the further laser enhanced hyperbaric underwater welding experiment.

**Key words:** laser enhanced; metal transfer; high-speed photograph; experiment

### Study on the softening of 6005A-T6 aluminum alloy welding joints for high-speed train

LÜ Xiaochun<sup>1</sup>, LEI Zhen<sup>1</sup>, ZHANG Jian<sup>1</sup>, ZHANG Lihua<sup>2</sup> (1. Harbin Welding Institute, China Academy of Machinery Science & Technology, Harbin 150028, China; 2. XCMG Construction Machinery Co., Ltd. Building Machinery Co., Xuzhou 221004, China). pp 25 – 29

**Abstract:** Welding thermal cycle curves of 6005A-T6 aluminum alloy by using tandem MIG welding and laser-tandem MIG hybrid welding was tested individually. The softening of the welding joints was studied through welding thermal simulation

with heat treatment method. The test results demonstrated that the notable softening in HAZ began as long as the peak temperature of welding thermal cycle curve exceeded 260 °C, and the most serious softening in HAZ occurred while the peak temperature of welding thermal cycle curve was up to 350 °C. The unstable phase of  $\beta''$  and  $\beta'$ , the main strengthening phase of 6005A-T6 aluminum alloy, transformed to  $\beta$  (Mg<sub>2</sub>Si) which aggregated and grew to block was the main reason why the softening happened. The hardness of the joints in HAZ, where the peak temperature of welding thermal cycle curve was between 260 – 500 °C, could not recover totally through ageing treatment. The detention time beyond 260 °C on the thermal cycle curve of laser-tandem MIG hybrid welding joints was much shorter than that of tandem MIG welding joints, so that the softening of laser-tandem MIG hybrid welding joints was little slighter than that of tandem MIG welding joints.

**Key words:** high-speed train; 6005A aluminum alloy; laser hybrid welding; softening of welding joints

### An improved three-dimensional reconstruction algorithm for microelectronics assembly solder joint

ZHAO Huihuang<sup>1,2</sup>, WANG Yaonan<sup>1</sup>, SUN Yaqi<sup>2</sup>, WEI Shudi<sup>2</sup> (1. College of Electrical and Information Engineering, Hunan University, Hunan 410082, China; 2. Department of Computer Science, Hengyang Normal University, Hengyang 421008, China). pp 30 – 34, 42

**Abstract:** Solder joint three-dimensional (3D) reconstruction is one of the key research of microelectronic assembly quality 3D detection and control technology development. During the solder joint 3D reconstruction based on SFS theory, its 3D reconstruction becomes one of the key problems because of existing “high light area” on solder joint surface. In order to resolve the problem, at first, by analyzing the reflection items on solder joint surface, a reflection model is got for microelectronics solder joint according to the characteristics of joint surface and solder joint image. Then, by analyzing the formation principle of “high light area” and modifying the reconstruction result, an improved 3D reconstruction algorithm is proposed for microelectronics assembly solder joint. At last, the experimental results have shown that the “distortion” can be solved and the 3D shape based on the improved illumination model is more satisfactory in decreasing specular reflection influence than that of the traditional methods.

**Key words:** solder joint; microelectronics assembly; three-dimensional reconstruction; shape from shading

### Optimization of transition in stainless steel welding joints S-N curve breaking point

ZHU Guoren<sup>1</sup>, CHEN Song<sup>2</sup>, WANG Zhenbao<sup>2</sup> (1. Chain Transmission Institute, Jilin University, Changchun 130025, China; 2. Institute of Mechanical Science and Engineering, Jilin University, Changchun 130025, China). pp 35 – 38

**Abstract:** Based on the ladder method and the group method, the S-N curve of stainless steel welding fittings was drawn. According to comparing drawn S-N curve with the ladder